THE ASTROPHYSICAL JOURNAL, 525:368–374, 1999 November 1


# MAXIMUM ENERGIES OF SHOCK-ACCELERATED ELECTRONS IN YOUNG SHELL SUPERNOVA REMNANTS

STEPHEN P. REYNOLDS
Physics Department, North Carolina State University, Raleigh, NC 27695-8202; steve_reynolds@ncsu.edu
AND
JONATHAN W. KEOHANE[1]
North Carolina School of Science and Mathematics, Durham, NC 27715-2418; keohane@academic.ncssm.edu
*Received 1999 January 8; accepted 1999 June 22*

## ABSTRACT

Young supernova remnants (SNRs) are often assumed to be the source of cosmic rays up to energies approaching the slight steepening in the cosmic-ray spectrum at around 1000 TeV, known as the "knee." We show that the observed X-ray emission of 14 radio-bright shell remnants, including all five historical shells, can be used to put limits on $E_{\rm max}$, the energy at which the electron energy distribution must steepen from its slope at radio-emitting energies. Most of the remnants show thermal spectra, so any synchrotron component must fall below the observed X-ray fluxes. We obtain upper limits on $E_{\rm max}$ by considering the most rapid physically plausible cutoff in the relativistic electron distribution, an exponential, which is as sharp or sharper than found in any more elaborate models. This maximally curved model then gives us the highest possible $E_{\rm max}$ consistent with not exceeding observed X-rays. Our results are thus independent of particular models for the electron spectrum in SNRs. Assuming homogeneous emitting volumes with a constant magnetic field strength of 10 $\mu$G, no object could reach 1000 TeV, and only one, Kes 73, has an upper limit on $E_{\rm max}$ above 100 TeV. All the other remnants have limits at or below 80 TeV. $E_{\rm max}$ is probably set by the finite remnant lifetime rather than by synchrotron losses for remnants younger than a few thousand years, so that an observed electron steepening should be accompanied by steepening at the same energy for protons. More complicated, inhomogeneous models could allow higher values of $E_{\rm max}$ in parts of the remnant, but the emission-weighted average value, that characteristic of typical electrons, should obey these limits. The young remnants are not expected to improve much over their remaining lives at producing the highest energy Galactic cosmic rays; if they cannot, this picture of cosmic-ray origin may need major alteration.

*Subject headings:* acceleration of particles — shock waves — supernova remnants — supernovae: general — X-rays: ISM

## 1. INTRODUCTION

The Galactic population of cosmic rays is generally presumed to originate in supernova remnant (SNR) shock waves through first-order Fermi (diffusive) shock acceleration (see Blandford & Eichler 1987 and Jones & Ellison 1991 for reviews), at least up to the "knee" around 1000 TeV, where steepening begins to take place. The idea of a single source population is strengthened by recent observations by the JACEE collaboration (Asakimori et al. 1998), confirming the absence of spectral structure below 800 TeV. However, direct evidence for a supernova-remnant origin has essentially consisted only of the presence of electrons with energies up to about 10 GeV or so, producing synchrotron emission. There appears to be no unambiguous evidence for the presence of cosmic-ray protons and nuclei, although EGRET gamma-ray observations of a few supernova remnants (Esposito et al. 1996) have been interpreted as at least partly due to the decay of neutral pions produced by interactions of cosmic-ray protons with thermal gas (Drury, Aharonian, & Völk 1994; Sturner et al. 1997; Gaisser, Protheroe, & Stanev 1998; Baring et al. 1999). However, it is quite possible that the gamma rays originate from pulsars rather than from this process, and even if the gamma-ray emission can be shown to have a diffuse origin, the above calculations show that the observed gamma-ray spectra must involve at least some contribution from electron processes: nonthermal bremsstrahlung or inverse-Compton upscattering of cosmic microwave background photons.

If the EGRET observations do represent diffuse shock-related emission, we will finally have evidence for the presence of at least electrons at energies of 100 GeV or so. However, X-ray observations of young supernova remnants (SN 1006, Koyama et al. 1995; Cas A, Allen et al. 1997; RX J1713.7−3946, Koyama et al. 1997; IC 443, Keohane et al. 1997) have revealed nonthermal components, which generally have been interpreted as synchrotron radiation from the high-energy tail of the electron distribution as it rolls off at energies of 10 TeV and above. The presence of electrons at such extreme energies was essentially confirmed for the remnant of SN 1006 by the discovery of TeV gamma rays (Tanimori et al. 1998), well described by the upscattering of cosmic microwave background photons by electrons with energies of 10–100 TeV. Thus, we now have evidence for electrons, at least, at energies within 1 or 2 orders of magnitude of the "knee," although some steepening from the radio spectrum must already have occurred.

Electrons and ions at low energies are treated quite differently in the shock-acceleration process. The "thermal leakage" model of ion injection, in which the highest energy

[1] This work was conducted while the author was affiliated with NASA/Goddard Space Flight Center and the University of Minnesota.

thermal ions are naturally "injected" into the Fermi process, seems to describe ion acceleration adequately (Jones & Ellison 1991), but electron injection is still a serious problem (Levinson 1992). From energies of 1 MeV to above 1 GeV, electrons and ions have markedly different spectra (Ellison & Reynolds 1991). However, well above 1 GeV per nucleon, all particles are extremely relativistic and are treated identically by the shock (as long as magnetohydrodynamic [MHD] waves of both helicities are available to scatter particles of both signs of charge). While the spectra are curved below 1 GeV, they assume the asymptotic logarithmic slope given by the simple test-particle formula (for the appropriate shock compression ratio, which may be larger than 4) well above 1 GeV. Both electron and ion distributions should be close to power laws with the same slope from energies above about 10 GeV or so until some maximum energy resulting from the finite time available for acceleration, radiative losses, or particle escape (Reynolds 1996, 1998; Gaisser et al. 1998; Sturner et al. 1997; Baring et al. 1999).

At these very high energies, then, the acceleration process should operate identically for electrons and ions. The one exception to this is a cutoff due to radiative losses on electrons. Once the rate of synchrotron and inverse-Compton energy losses ($\propto E^2$) becomes equal to the rate of energy gain by shock acceleration, further electron acceleration will cease and the electron distribution will cut off exponentially (Webb, Drury, & Biermann 1984). Other processes, such as a finite age of the shock, or a change in the nature of scattering above some energy due to absence of long-wavelength MHD waves, can also cause cutoffs in the power-law spectra. Either of these latter processes should affect electrons and ions equally, so a cutoff in the electron distribution would also imply a cutoff at the same energy in the proton distribution.

In all the observed cases of nonthermal X-ray emission in SNRs, it is clear that the electron spectrum must have begun to steepen considerably below X-ray–emitting energies, because the X-ray fluxes lie well below the extrapolation of the radio spectrum. Thus, any X-rays, nonthermal or not, can put limits on the maximum energy to which electrons can have been accelerated in a remnant. The quantitative elaboration of this simple idea is the point of our paper. The unobserved proton spectrum could extend to higher energies before steepening, if it can be shown that the electron spectrum is limited by radiative losses; otherwise, a limit on the electron maximum energy is a limit on the proton maximum energy.

We selected a sample of 14 Galactic remnants, including all five shell remnants of historical supernovae, to test this idea. Our list comprises 11 of the top 12 Galactic remnants in radio surface brightness, as well as those ranked 21 and 22. This sample includes the brightest remnants that both are smaller than 10′ in diameter and have public *ASCA* data, plus the remnant of SN 1006 AD. Table 1 shows our sample in order of decreasing radio surface brightness, with each object's radio flux, mean surface brightness, X-ray count rate, and radio flux extrapolated to $10^{17}$ Hz ($\sim$3 keV). The extrapolated flux is derived from the radio flux and spectral index; it represents what the synchrotron emission in the X-ray would be in the absence of any electron spectral steepening.

Our strategy will be to find the upper limit to $E_{\max}$ by assuming that each remnant contains a maximally curved nonthermal component. We emphasize that we do not assert that this component is physically required for these objects, simply that its value for the cutoff frequency is the highest allowable by the data. We do not propose to produce physical models for these objects. In particular, the various assumptions involved in a recent collection of models for nonthermal X-rays from SNRs (Reynolds 1998) are not required here. That work attempts to describe potentially observable synchrotron X-ray emission; here we require only upper limits. Our results show that while young SNRs are likely to be the primary source of cosmic rays below the "knee," they cannot be used to explain the CR spectrum above the knee, or perhaps even that far.

We stress that our limits do not depend on a particular detailed model for the shape of the electron spectrum, since we have chosen a maximally curved model. Many calcu-

TABLE 1

TOP RADIO SURFACE BRIGHTNESS SHELL-TYPE SNRS IN THE MILKY WAY SMALLER THAN 10′ IN DIAMETER THAT HAVE PUBLIC *ASCA* DATA

| RANK IN $\Sigma$ | NAME(S) | 1 GHz FLUX (Jy) | $\Sigma$ AT 1 GHz (Jy arcmin$^{-2}$) | MPC RATE (counts s$^{-1}$) | EXTRAPOLATED 1 keV FLUX DENSITY | |
|---|---|---|---|---|---|---|
| | | | | | (mJy) | (photons s$^{-1}$ cm$^{-2}$ keV$^{-1}$) |
| 1 ..... | Cas A | 2720 | 140 | 109 | 0.9 | 1.5 |
| 2 ..... | G349.7+0.2 | 20 | 5.1 | N/A | 1.3 | 2.0 |
| 3 ..... | W49 B | 38 | 4.0 | 4.7 | 3.5 | 5.6 |
| 4 ..... | Kepler | 19 | 2.7 | 4.5 | 0.08 | 0.13 |
| 5 ..... | 3C 397 | 22 | 2.5 | 2.5 | 2.0 | 3.2 |
| 6 ..... | SN 386[a] | 22 | 1.8 | 1.8 | 1.7 | 2.7 |
| 7 ..... | Tycho | 56 | 1.1 | 27.5 | 0.4 | 0.7 |
| 8 ..... | 3C 391 | 24 | 0.9 | 1.4 | 0.6 | 0.9 |
| 10..... | 3C 396 | 18 | 0.5 | 0.6 | 0.2 | 0.3 |
| 11..... | Kes 73[a] | 6 | 0.5 | 4.7 | 0.01 | 0.02 |
| 12..... | RCW 103[a] | 28 | 0.4 | 4.4 | 1.8 | 2.8 |
| 21..... | G346.6−0.2 | 10 | 0.2 | N/A | 0.6 | 1.0 |
| 22..... | G352.7−0.1 | 4 | 0.2 | N/A | 0.04 | 0.06 |

NOTE.—Sources of information are Green's catalogue (Green 1988) and Seward (1990).

[a] While classified as shell-type by Green, these SNRs have known central sources.

lations of particle spectra produced in shocks of finite age and subject to radiative, adiabatic, and other losses have been performed (e.g., Kardashev 1962; Webb, Drury, & Biermann 1984; Drury 1991; Kang & Jones 1991; Ellison & Reynolds 1991; Berezhko, Elshin, & Ksenofontov 1996; Reynolds 1996, 1998; Berezhko & Völk 1997; Gaisser et al. 1997; Sturner et al. 1997; Baring et al. 1999; etc.). In no case does a calculation produce a spectral cutoff faster than exponential. Thus, we obtain the most conservative upper limit on $E_{\max}$ by considering the synchrotron spectrum due to an exponential cutoff, which will then allow a higher cutoff energy before violating observed X-ray fluxes than any realistic model. We hope in this way to avoid discussions of the merits of different models for accelerated-particle spectra, and we believe that our results are completely general.

## 2. METHOD OF ANALYSIS

### 2.1. *The Data*

To get upper limits on the energy at which the electron spectrum must begin to break, we used the fastest plausible cutoff, an exponential. It can be shown for either acceleration-time limits (Drury 1991) or radiative-loss limits (Webb, Drury, & Biermann 1984) that particle spectra cut off roughly exponentially, within 10% or so for the time-limited case (L. O'C. Drury 1991, private communication). We therefore assume an electron spectrum of the form

$$N_e(E) = KE^{-s}e^{-E/E_{\max}} . \quad (1)$$

The most rapid possible synchrotron cutoff is then obtained by folding this distribution through the single-particle synchrotron emissivity, assuming a constant magnetic field. This maximally sharp synchrotron cutoff is shown in Figure 1, along with an exponential photon distribution, which would result from an abruptly truncated electron distribution, and an approximation to the volume emissivity of the exponentially cut off electron spectrum. The actual emissivity is far above that of the truncated distribution, and considerably above the approximate version at energies well above the characteristic cutoff frequency $\nu_m$. We used the numerically calculated version below. Note that any inhomogeneity in the remnant, such as varying magnetic field strength or varying the constant $K$ in equation (1), will broaden the total spectrum. Our assumptions should permit the highest possible value of $E_{\max}$ for any observed X-ray spectrum.

The decrement function (the ratio of the actual emissivity to the power-law extrapolation) is also shown in Figure 1; it is a one-parameter function that was embedded into XSPEC for fitting. The total nonthermal spectrum can then be characterized by three parameters:

1. The 1 GHz radio flux density, $S_{1\mathrm{GHz}}$.
2. The radio spectral index, $\alpha$ ($s = 2\alpha + 1$).
3. The rolloff frequency, $\nu_{\mathrm{rolloff}}$.

Two of these parameters, $S_{1\mathrm{GHz}}$ and $\alpha$, are radio-derived quantities and have been well measured over the years. In fact, both of these quantities are compiled in Green's catalog (Green 1988). Therefore, this simplistic model yields a photon spectrum parameterized only by the radio spectrum and a maximum "rolloff frequency." The rolloff frequency is related to the cutoff electron energy via the relation

$$\nu_{\mathrm{rolloff}} \approx 0.5 \times 10^{16}\left(\frac{B}{10\ \mu\mathrm{G}}\right)\left(\frac{E_{\max}}{10\ \mathrm{TeV}}\right)^2 . \quad (2)$$

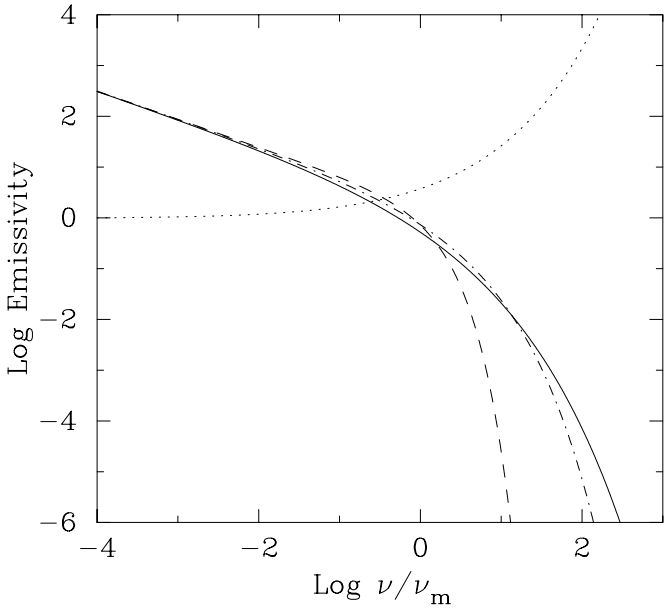


FIG. 1.—Synchrotron emissivity produced by the electron spectrum of eq. (1), with power-law index $s = 2$. The solid line shows the numerical integration of the single-particle emissivity; the dashed line shows the emissivity of an abruptly truncated electron distribution [$N(E) = 0$ for $E > E_{\max}$], and the dot-dashed line shows the distribution of eq. (1) convolved with the $\delta$-function approximation to the single-particle synchrotron emissivity. The dotted line shows the log of inverse of the decrement function, the factor by which the cutoff emissivity lies below the power-law extrapolation.

The analysis of all the SNRs presented in this chapter (except for Cas A) uses archival Gas Imaging Spectrometer (GIS) data from the *ASCA* observatory, and takes advantage of the recent Revision 2 batch data analysis (Pier 1997). For each *ASCA* pointing, the data are screened and spectra are extracted from circular regions around the sources in the field of view. These spectra, along with their accompanying response functions, are provided with the Revision 2 data. Background spectra, however, are not provided in the standard processing.

For each SNR presented here, the extraction region of the standard processing was verified as encompassing the SNR. In each case, the Revision 2 regions encompassed the SNR but excluded unnecessary excess background—just as one would draw them by hand.

Background spectra were produced by excluding the sources by hand from the Revision 2 screened event files and extracting the leftover events. This was possible because only SNRs smaller than 10′ were included in this sample.

### 2.2. *The Spectral Fitting Methods*

The spectra of each of these SNRs (including Cas A) were fitted with our simple maximally curved model plus "narrow" Gaussian emission lines. When necessary, an

TABLE 2

ROLLOFF FREQUENCY AND MAXIMUM ELECTRON ENERGY UPPER LIMITS

| OBJECT | $\nu_{rolloff}$ ($10^{16}$ Hz) | $\nu_{rolloff}$ (keV) | $E_{max}[(B/10\mu G)]^{1/2}$ (ergs) | $E_{max}[(B/10\mu G)]^{1/2}$ (TeV) |
|---|---|---|---|---|
| Kes 73[a] ..... | 150 | 6 | 290 | 200 |
| Cas A..... | 32 | 1 | 130 | 80 |
| Kepler ..... | 11 | 0.5 | 79 | 50 |
| Tycho ..... | 8.8 | 0.4 | 70 | 40 |
| G352.7−0.1..... | 6.6 | 0.3 | 60 | 40 |
| SN 1006[b]..... | 6 | 0.2 | 57 | 40 |
| 3C 397..... | 3.4 | 0.1 | 43 | 30 |
| W49 B..... | 2.4 | 0.1 | 36 | 20 |
| G349.7+0.2..... | 1.8 | 0.07 | 31 | 20 |
| 3C 396..... | 1.6 | 0.07 | 30 | 20 |
| G346.6−0.2..... | 1.5 | 0.06 | 29 | 20 |
| 3C 391..... | 1.4 | 0.06 | 28 | 20 |
| SN 386[a] ..... | 1.2 | 0.05 | 26 | 20 |
| RCW 103[a] ..... | 1.2 | 0.05 | 26 | 20 |

NOTE.—Values shown in this table are upper limits, because in each case the bulk of the continuum is assumed to be synchrotron. Values shown in cgs units were rounded to two digits, while their common-unit equivalents were rounded to the more reasonable one significant figure. Note that while 10 $\mu$G was assumed for a standard SNR magnetic field, Cas A's magnetic field is about 1 mG (i.e., $E_{max} \sim 8$ TeV), and others are quite uncertain.

[a] Contains a known hard X-ray central source.

[b] This value of $\nu_{rolloff}$ is not a limit but results from the model of the nonthermal X-ray emission by Reynolds (1996). See § 4.

TABLE 3

BEST-FIT UPPER LIMIT ON THE ROLLOFF FREQUENCY ($\nu_{rolloff}$) FOR CAS A WITH X-RAY SPECTRUM ABOVE 10 keV PRODUCED EXCLUSIVELY BY SYNCHROTRON RADIATION

| Parameter | Value | Source |
|---|---|---|
| Absorption Model | | |
| $N_H$ ..... | $1 \times 10^{22}$ cm$^{-2}$ | |
| Synchrotron Model | | |
| $S_{1GHz}$ ..... | 2720 Jy | Green (1988) |
| $\alpha$..... | 0.77 | Green (1988) |
| max $\nu_{rolloff}$ ..... | $3.15 \times 10^{17}$ Hz | This *RXTE* fit |

NOTE.—That the X-ray spectrum above 10 keV is produced exclusively by synchrotron radiation is probably a good assumption for Cas A (Allen et al. 1997). This fit had $\chi^2 = 290$ for 105 degrees of freedom. In addition, the normalization was allowed to float on only the HEXTE component (higher energy spectrum) to account for well-known problems with early HEXTE calibration. The spectrum is shown in Figure 2.

TABLE 4

BEST-FIT ROLLOFF FREQUENCY OF CAS A ($\times 10^{16}$ Hz) AS A FUNCTION OF RADIO FLUX DENSITY AND SPECTRAL INDEX

| $\alpha$ | $S_{1GHz}$ 2700 Jy | 2710 Jy | 2720 Jy | 2730 Jy | 2740 Jy |
|---|---|---|---|---|---|
| 0.62..... | 4.6 | 4.6 | 4.6 | 4.6 | 4.6 |
| 0.67..... | 7.7 | 7.7 | 7.7 | 7.6 | 7.6 |
| 0.72..... | 14 | 14 | 14 | 14 | 14 |
| 0.77..... | 32 | 32 | 31.5 | 31 | 31 |
| 0.82..... | 95 | 95 | 95 | 94 | 94 |
| 0.87..... | 610 | 600 | 600 | 590 | 590 |

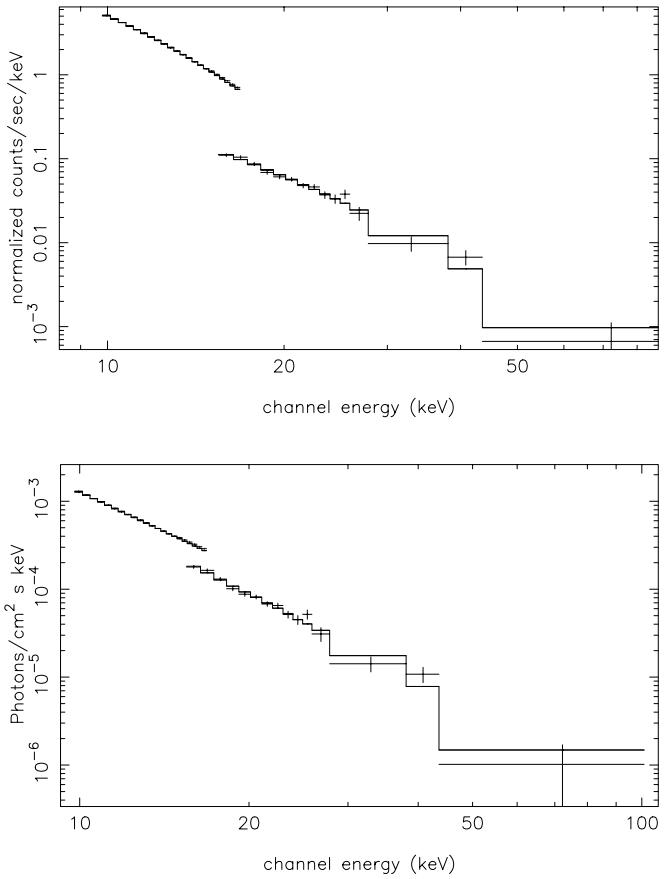


FIG. 2.—Folded (*top*) and unfolded (*bottom*) *RXTE* spectra of Cas A with the parameters given in Table 3 used in the fit.

additional soft thermal bremsstrahlung component was added, and in a few cases a very hard power-law component was added to account for excess emission above 7 keV. Naturally, the standard Wisconsin absorption (Morrison & McCammon 1983) was applied to all *ASCA* fits.

## 3. RESULTS

The results of this analysis are summarized in Table 2. For two representative remnants, we show the detailed model fits in tables and figures, where we display both folded spectra in counts s$^{-1}$ keV$^{-1}$ and (nonuniquely) unfolded spectra in photons cm$^{-2}$ s$^{-1}$ keV$^{-1}$. Below, we comment on these two objects. Complete details on the fits for all 13 objects (excepting SN 1006) can be found in Keohane (1998).

### 3.1. *Cassiopeia A*

Unlike all the other SNRs in our sample, Cas A has been observed by *RXTE* and the data have been analyzed (Allen et al. 1997). Here we fit the *RXTE* spectrum of Cas A with our simple synchrotron model alone, resulting in a good fit to both the PCA and HEXTE data (Tables 3 and 4 and Fig. 2). These result in a maximum electron value of 80 TeV for our nominal magnetic field of 10 $\mu$G; for Cas A, this is almost certainly an underestimate, resulting in a lower value of $E_{max}$.

### 3.2. *W49 B*

In order to obtain an upper limit to the synchrotron

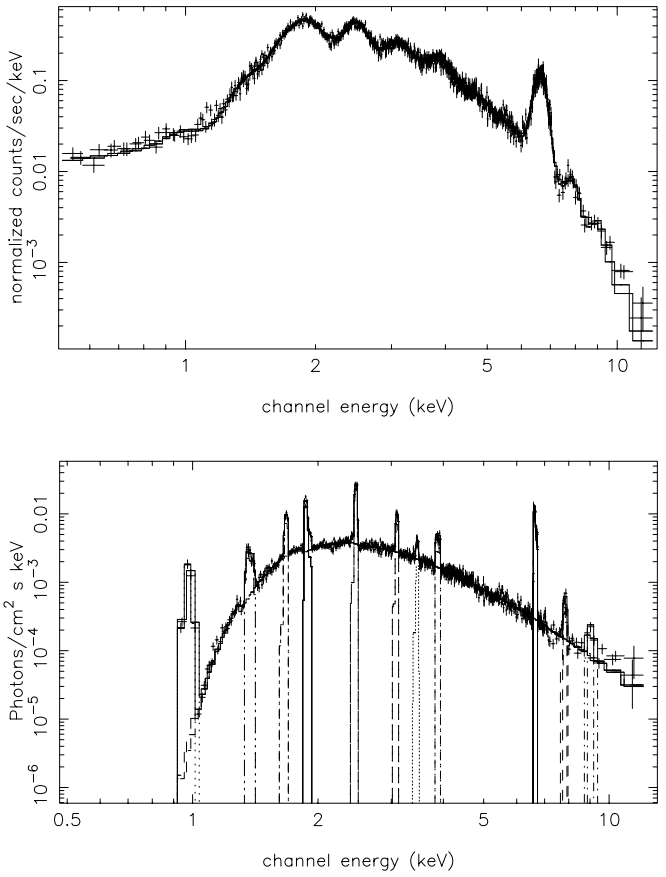


FIG. 3.—Folded (*top*) and unfolded (*bottom*) spectra of W49 B with the parameters given in Table 5 used in the fit.

emission from W49 B, the 95 ks spectrum was fitted assuming that the 0.5–12.0 keV continuum is entirely synchrotron. Our synchrotron model was used to fit the continuum, and no other continuum component was required. A plot of the *ASCA* GIS spectrum with this model fit is shown in Figure 3, and the model parameters are presented in Tables 5 and 6.

### 3.3. *SN 1006*

One historical shell remnant, that of the supernova of A.D. 1006, has too low a radio surface brightness, and is too large, to qualify for our sample. However, SN 1006 is the one SNR whose X-ray spectrum is known to be actually produced by synchrotron radiation. While its spectrum rolls off more slowly than our maximally curved spectrum due to inhomogeneities, we can treat the calculated $\nu_m$ of the model (Reynolds 1996) as equivalent to the upper limits we quote for the rest of the remnants. This value is included in Table 2.

## 4. DISCUSSION

The results of these fits are shown in Table 2. Our fiducial magnetic field strength of 10 $\mu$G is merely an estimate; since $E_{\max} \propto (\nu_m/B)^{1/2}$, our maximum energies are relatively insensitive to the fitted $\nu_m$ and to the magnetic field.

We see that in all cases (except Kes 73, which is unusual, containing a central source), the electron spectrum has begun to roll off at energies well below 100 TeV. This is not in conflict with direct observations of cosmic-ray electrons. We do not have any direct evidence for cosmic-ray electrons of 1000 TeV; in fact, the cosmic-ray electron spectrum at Earth is already considerably steeper than that of cosmic-ray protons by 1 TeV (e.g., Golden et al. 1984). However, as described in § 1, unless the electron rolloff is due to radiative losses, the proton spectrum should not extend beyond the electron spectrum, and none of these remnants could produce cosmic-ray protons anywhere close to the "knee." The low values of $E_{\max}$, and the disturbing implications for

TABLE 5

BEST-FIT SPECTRUM OF W49 B ASSUMING SYNCHROTRON RADIATION AS PRIMARY SOURCE OF X-RAY CONTINUUM EMISSION

| Parameter | Value |
|---|---|
| **Absorption Component** | |
| $N_H$ ..... | $4.1 \times 10^{22}$ cm$^{-2}$ |
| **Synchrotron Component** | |
| $S_{1\,GHz}$ ..... | 38 Jy |
| $\alpha$ ..... | 0.5 |
| max $\nu_{rolloff}$ ..... | $2.5 \times 10^{16}$ Hz |
| **Narrow Gaussian Components** | |
| 1. $F_{line}$ ..... | 3.7 photons cm$^{-2}$ s$^{-1}$ |
| Line Energy..... | 0.97 keV |
| 2. $F_{line}$ ..... | $1.3 \times 10^{-2}$ photons cm$^{-2}$ s$^{-1}$ |
| Line Energy..... | 1.4 keV |
| 3. $F_{line}$ ..... | $3.9 \times 10^{-3}$ photons cm$^{-2}$ s$^{-1}$ |
| Line Energy..... | 1.7 keV |
| 4. $F_{line}$ ..... | $5.0 \times 10^{-3}$ photons cm$^{-2}$ s$^{-1}$ |
| Line Energy..... | 1.9 keV |
| 5. $F_{line}$ ..... | $3.0 \times 10^{-3}$ photons cm$^{-2}$ s$^{-1}$ |
| Line Energy..... | 2.5 keV |
| 6. $F_{line}$ ..... | $6.7 \times 10^{-4}$ photons cm$^{-2}$ s$^{-1}$ |
| Line Energy..... | 3.1 keV |
| 7. $F_{line}$ ..... | $1.6 \times 10^{-4}$ photons cm$^{-2}$ s$^{-1}$ |
| Line Energy..... | 3.5 keV |
| 8. $F_{line}$ ..... | $4.3 \times 10^{-4}$ photons cm$^{-2}$ s$^{-1}$ |
| Line Energy..... | 3.9 keV |
| 9. $F_{line}$ ..... | $1.2 \times 10^{-3}$ photons cm$^{-2}$ s$^{-1}$ |
| Line Energy..... | 6.6 keV |
| 10. $F_{line}$ ..... | $8 \times 10^{-5}$ photons cm$^{-2}$ s$^{-1}$ |
| Line Energy..... | 7.8 keV |
| 11. $F_{line}$ ..... | $5 \times 10^{-5}$ photons cm$^{-2}$ s$^{-1}$ |
| Line Energy..... | 9.0 keV |

NOTE.—This fit had $\chi^2 = 996$ for 835 degrees of freedom ($\chi^2_\nu = 1.2$). The radio flux and spectral index are taken from Green (1988) and frozen in the X-ray fit. The spectrum is shown in Figure 3.

TABLE 6

BEST-FIT ROLLOFF FREQUENCY OF W49 B ($\times 10^{16}$ Hz) AS A FUNCTION OF RADIO FLUX DENSITY AND SPECTRAL INDEX

| | $S_{1\,GHz}$ | | | | |
|---|---|---|---|---|---|
| $\alpha$ | 36 Jy | 37 Jy | 38 Jy | 39 Jy | 40 Jy |
| 0.40..... | 1.1 | 1.1 | 1.0 | 1.0 | 1.0 |
| 0.45..... | 1.6 | 1.6 | 1.5 | 1.5 | 1.5 |
| 0.50..... | 2.5 | 2.5 | 2.5 | 2.4 | 2.4 |
| 0.55..... | 4.4 | 4.3 | 4.2 | 4.2 | 4.1 |
| 0.60..... | 8.9 | 8.7 | 8.5 | 8.4 | 8.2 |

cosmic-ray acceleration in young remnants, form the primary result of this work.

There are possible loopholes in this argument. The most straightforward way out is by invoking the $B$-dependence of our inferred $E_{\max}$. But magnetic field strengths would need to be absurdly low (less than 0.1 $\mu$G) to get $E_{\max}$ up to 1000 TeV. This seems exceptionally unlikely.

Young remnants have a maximum nonthermal particle energy that is limited by the finite time available for acceleration; as they age, that limit obviously rises, while the radiative-loss limit on electrons decreases. Unless particle escape intervenes, older remnants are likely to be loss-limited after a few thousand years (Reynolds 1998). The older remnants in our sample might be loss-limited, so that the proton spectrum could extend well beyond the $E_{\max}$ values we report. However, at the cost of introducing some model dependence, it is possible to calculate the maximum energy allowed by synchrotron (and inverse-Compton) losses (Lagage & Cesarsky 1983; Reynolds 1998). That energy depends on the obliquity angle, $\theta_{B,n}$, between the shock normal and the upstream magnetic field, as well as on the shock compression ratio, the "gyrofactor" $\eta$ (ratio of mean free path to gyroradius), and the shock velocity (Reynolds 1998, eq. [14]). The assumption that the diffusion coefficient scales with particle energy is sensible and widely made, and can accommodate a wide range of conditions (e.g., strong turbulence, $\eta = 1$). Then the cutoff frequency corresponding to this maximum energy, $E_{\max}(\mathrm{loss})$, will be roughly $\nu_m(\mathrm{loss}) = 5.4 \times 10^{18}\, B_1\, E^2_{\max}(\mathrm{loss})$, where $B_1$ is the upstream magnetic field strength and we have assumed a factor of 3 compression as a rough average over the remnant. For electron acceleration with a diffusion coefficient proportional to energy (i.e., to gyroradius), as assumed here, it turns out that $E_{\max}(\mathrm{loss}) \propto B^{-1/2}$, so the synchrotron break frequency due to losses does not depend on $B$, but only on the shock velocity. Since most of a remnant's shock surface will encounter nearly perpendicular shocks ($\theta_{B,n} \geq 45^\circ$), we take $\theta_{B,n} = 90^\circ$ for an estimate. For a shock-compression ratio of 4, the result is

$$\nu_m(\mathrm{loss}) = 4.9 \times 10^{16}\left(\frac{1+\eta^2}{\eta}\right) u_8^2 \ \mathrm{Hz}\ , \qquad (3)$$

where $u_8 \equiv u_{\mathrm{sh}}/10^8$ cm s$^{-1}$. We get the lowest value for $\eta = 1$, so

$$\nu_m(\mathrm{loss}) = 9.9 \times 10^{16}\, u_8^2 \ \mathrm{Hz}\ . \qquad (4)$$

However, five of our objects are associated with historical supernovae within the last 2000 yr. Table 7 lists those objects, along with shock velocities estimated from X-ray observations, proper motions, and other means. We are thus able to predict fairly firm lower limits to the frequency corresponding to the cutoff energy for the dominant electron population. Those lower limits are given in Table 7, along with the observed limits from Table 2. In all five cases, it appears that the observed break is lower than the lower limit of what losses can produce, by about an order of magnitude. Thus, the spectral steepening must be due not to losses, but to finite age, so that the inferred $E_{\max}$ should apply to protons as well.

If the acceleration is age-limited in these objects, acceleration to higher energies will be possible as the remnants grow older. However, the maximum energy rises slowly. Once a remnant is in the Sedov phase, assumed to begin at time $t_{\mathrm{S}}$, the maximum energy will rise above $E_{m,\mathrm{S}} \equiv E_{\max}(t_{\mathrm{S}})$ according to

$$E_{\max} = 5E_{m,\mathrm{S}}[1 - (t/t_{\mathrm{S}})^{-1/5}] \leq 5E_{m,\mathrm{S}}\ , \qquad (5)$$

which will not provide much help. Only Cas A is likely to be close to free expansion still; proper-motion expansion rates for Kepler, Tycho, and SN 1006 (see Moffett, Goss, & Reynolds 1993 for a summary) show that these three objects are well into the transition to Sedov dynamics.

TABLE 7

COMPARISON OF OBSERVED ROLLOFF FREQUENCY UPPER LIMITS FROM TABLE 2 WITH THEORETICAL LOWER LIMITS TO A ROLLOFF FREQUENCY CAUSED BY SYNCHROTRON LOSSES

| Object | $\nu_{m16}$ (observed) ($10^{16}$ Hz) | $u_8$[a] | $\nu_{m16}$ (losses) ($10^{16}$ Hz) | Reference |
|---|---|---|---|---|
| Cas A ..... | 32 | 5 | 300 | 1 |
| Kepler ..... | 11 | 2.5 | 60 | 2 |
| Tycho ..... | 8.8 | 2.5 | 60 | 3 |
| SN 1006..... | 6 | 3.1 | 100 | 3 |
| SN 386 ..... | 1.2 | 1 | 10 | 4 |

[a] Here $u_8 \equiv u_{\mathrm{sh}}/1000$ km s$^{-1}$. Shock velocities are approximate and are derived typically from optical observations.

REFERENCES.—(1) Kirshner & Chevalier 1978; (2) Borkowski, Blondin, & Sarazin 1992; (3) Smith et al. 1991; (4) Reynolds et al. 1994.

## 5. CONCLUSION

No Galactic supernova remnant has X-ray emission bright enough to lie on the extrapolation of its radio spectrum. Thus, the spectrum of electrons responsible for the radio emission must steepen or cut off before reaching X-ray–emitting energies. We derive upper limits to the cutoff energies using the most sharply cut off physically reasonable model, the synchrotron emissivity of a power-law electron spectrum with an exponential cutoff. Those upper limits are listed in Table 2 for 14 remnants with some of the highest radio surface brightnesses in the Galaxy. In all cases, the electron spectrum must steepen well below the "knee" in the cosmic-ray spectrum at around $10^{15}$ eV (1000 TeV). We see four possibilities: (1) These remnants are not producing current cosmic rays (but may in the future as they age). (2) Their electron spectra cut off sooner than their proton spectra (but this should not be true for the five historical remnants). (3) We fundamentally do not understand some important feature of particle acceleration that can discriminate between electrons and protons even at energies of 1 TeV and above. (4) SNRs do not produce Galactic cosmic rays even to within an order of magnitude of the "knee."

We stress that the fundamental source of the limits, the fact that all SNRs in our sample are fainter in X-rays than the extrapolated radio spectrum, is completely model-independent. We have taken the sharpest possible physically reasonable cutoff in the electron spectrum to find the highest frequency at which the electron spectrum could begin to cut off and still not exceed the observed X-rays. There is a bit of model dependence in our assertion that the five historical shells have break frequencies too low to be caused by synchrotron losses; here we used very standard shock-acceleration theory, but less standard assumptions (a different energy dependence of the diffusion coefficient, for instance) might allow radiative losses to produce the break, so that it would apply to electrons only. However, we

emphasize that our limits are limits; the true turnover frequencies could be still lower.

We plan to extend this work as new X-ray observations become available. Cruder limits can be obtained from integrated X-ray flux observations of older, larger remnants, and we intend to attempt this. However, these results should cause some discomfort in the particle-acceleration community. If our 14 objects are typical of the supernova remnants that produce cosmic rays, the canonical picture of Galactic cosmic-ray origin may need substantial revision.

## REFERENCES


Allen, G. E., et al. 1997, ApJ, 487, L97
Asakimori, K., et al. 1998, ApJ, 502, 278
Baring, M. G., Ellison, D. C., Reynolds, S. P., Grenier, I., & Goret, P. 1999, ApJ, 513, 311
Berezhko, E. G., Elshin, V. K., & Ksenofontov, L. T. 1996, Astron. Rep., 40, 155
Berezhko, E. G., & Völk, H. J. 1997, Astropart. Phys., 7, 183
Blandford, R. D., & Eichler, D. 1987, Phys. Rep., 154, 1
Borkowski, K. J., Blondin, J. M., & Sarazin, C. L. 1992, ApJ, 400, 222
Drury, L. O'C. 1991, MNRAS, 251, 340
Drury, L. O'C., Aharonian, F. A., & Völk, H. J. 1994, A&A, 287, 959
Ellison, D. C., & Reynolds, S. P. 1991, ApJ, 382, 242
Esposito, J. A., Hunter, S. D., Kanbach, G., & Sreekumar, P. 1996, ApJ, 461, 820
Gaisser, T. K., Protheroe, R. J., & Stanev, T. 1998, ApJ, 492, 219
Golden, R. L., Mauger, B. G., Badhwar, G. D., Daniel, R. R., Lacy, J. L., Stephens, S. A., & Zipse, J. E. 1984, ApJ, 287, 622
Green, D. A. 1988, Ap&SS, 148, 3
Jones, F. C., & Ellison, D. C. 1991, Space Sci. Rev., 58, 259
Kang, H., & Jones, T. W. 1991, MNRAS, 249, 439
Kardashev, N. S. 1962, Soviet Astron.—AJ, 6, 317
Keohane, J. W. 1998, Ph.D. thesis, Univ. Minnesota
Keohane, J. W., Petre, R., Gotthelf, E. V., Ozaki, M., & Koyama, K. 1997, ApJ, 484, 350
Kirshner, R. P., & Chevalier, R. A. 1978, ApJ, 233, 154
Koyama, K., Kinugasa, K., Matsuzaki, K., Nishiuchi, M., Sugizaki, M., Torii, K., Yamauchi, S., & Aschenbach, B. 1997, PASJ, 49, L7
Koyama, K., Petre, R., Gotthelf, E. V., Hwang, U., Matsuura, M., Ozaki, M., & Holt, S. S. 1995, Nature, 378, 255
Lagage, P.-O., & Cesarsky, C. J. 1983, A&A, 125, 249
Levinson, A. 1992, ApJ, 401, 73
Moffett, D. A., Goss, W. M., & Reynolds, S. P. 1993, AJ, 106, 1566
Morrison, R., & McCammon, D. 1983, ApJ, 270, 119
Pier, E. A. 1997, *ASCA*: Getting Started Guide for Revision 2 Data (Version 6.1; Greenbelt, MD: NASA/Goddard Space Flight Center)
Reynolds, S. P. 1996, ApJ, 459, L13
———. 1998, ApJ, 493, 375
Reynolds, S. P., Lyutikov, M., Blandford, R. D., & Seward, F. D. 1994, MNRAS, 271, L1
Seward, F. D. 1990, ApJS, 73, 781
Smith, R. C., Kirshner, R. P., Blair, W. P., & Winkler, P. F. 1991, ApJ, 375, 652
Sturner, S. J., Skibo, J. G., Dermer, C. D., & Mattox, J. R. 1997, ApJ, 490, 619
Tanimori, T., et al. 1998, ApJ, 497, L25
Webb, G. M., Drury, L.O'C., & Biermann, P. L. 1984, A&A, 137, 185